

## The Reaction Mechanism for the Organocatalytic Ring-Opening Polymerization of L-Lactide Using a Guanidine-Based Catalyst: Hydrogen-Bonded or Covalently Bound?

Anthony Chuma,<sup>†</sup> Hans W. Horn,<sup>†</sup> William C. Swope,<sup>†</sup> Russell C. Pratt,<sup>‡</sup> Lei Zhang,<sup>§</sup>  
Bas G. G. Lohmeijer,<sup>¶</sup> Charles G. Wade,<sup>†</sup> Robert M. Waymouth,<sup>#</sup>  
James L. Hedrick,<sup>†</sup> and Julia E. Rice<sup>\*,†</sup>

IBM Almaden Research Center, 650 Harry Road, San Jose, California 95032, Seeo, Inc.,  
Berkeley, California 94710, Department of Chemistry, University of North Carolina at Chapel  
Hill, Chapel Hill, North Carolina 27599, BASF SE, Global Polymer Research Division,  
67056 Ludwigshafen, Germany, and Department of Chemistry,  
Stanford University, Stanford, California 94305

Received August 29, 2007; E-mail: julia@almaden.ibm.com

**Abstract:** We have investigated two alternative mechanisms for the ring-opening polymerization of L-lactide using a guanidine-based catalyst, the first involving acetyl transfer to the catalyst, and the second involving only hydrogen bonding to the catalyst. Using computational chemistry methods, we show that the hydrogen bonding pathway is considerably preferred over the acetyl transfer pathway and that this is consistent with experimental information.

### Introduction

There has been considerable interest recently in living polymerization reactions that can be used to create polymers of predetermined molar mass with high end group fidelity and low polydispersity. This level of control is particularly useful in the formation of interesting and functional microstructures, such as diblock copolymers. At our facility, there has been focus on the development of metal-free organocatalytic ring-opening polymerizations of cyclic esters. Traditionally, the catalysts for the ring-opening polymerization (ROP) have been based on metals.<sup>1</sup> However, these catalysts are not ideal for electronic or medical applications since the residual metals may affect the quality of the product. The first organocatalytic study at IBM Almaden demonstrated that stabilized cyclic carbenes were effective catalysts for cyclic esters with turnover frequencies as high as 18 per second.<sup>2</sup> The second class of organocatalysts investigated was the bifunctional thiourea amines. These catalysts achieved polydispersities (<1.05) narrower than those of the N-heterocyclic carbenes, although, in general, the reaction times were longer.<sup>3</sup> More recently, we identified a bicyclic

guanidine-based catalyst, triazabicyclodecene (TBD), that shows controlled high activity for solution-phase ROP of cyclic esters.<sup>4,5</sup>

Understanding the reaction mechanism of the initial step of the ROP of L-lactide by TBD is clearly of benefit since it should allow us to design improved catalysts, suggest alternative reaction conditions (e.g., more or less polar solvents), and potentially aid in the design of reactants that enhance the enantiomeric purity of the product. Possible reaction mechanisms were discussed in all three studies based on the experimental findings,<sup>2–5</sup> but none were verified computationally. Thus, it is the purpose of this work to investigate the initial step of the TBD-catalyzed reaction using computational methods. However, in order to set the stage for the reaction schemes that we investigated, it is important to clarify some details of the experimentally proposed mechanisms for the three studies. First, the mechanisms for initial step of the N-heterocyclic carbenes and the TBD-catalyzed reactions were both assumed to involve direct covalent binding of the catalyst to the carbonyl group of the ester, with release of the catalyst in a later step.<sup>2,4,5</sup> This mechanism, involving direct covalent bonding as the first stage, is illustrated for the TBD reaction with L-lactide in Scheme 1. In this scheme, TBD inserts into the ester group of the L-lactide, and subsequent hydrogen bonding of the adjacent nitrogen to an incoming alcohol completes a transesterification cycle to form the polyester.

We chose to compare and contrast this to a hydrogen bonding mechanism (Scheme 2) that was inspired by the mechanism

<sup>†</sup> IBM Almaden Research Center.

<sup>‡</sup> Seeo, Inc.

<sup>§</sup> University of North Carolina at Chapel Hill.

<sup>¶</sup> BASF SE.

<sup>#</sup> Stanford University.

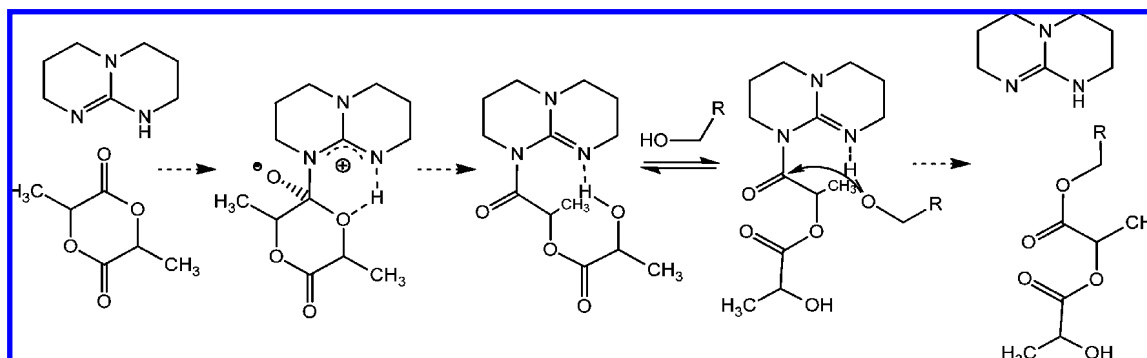
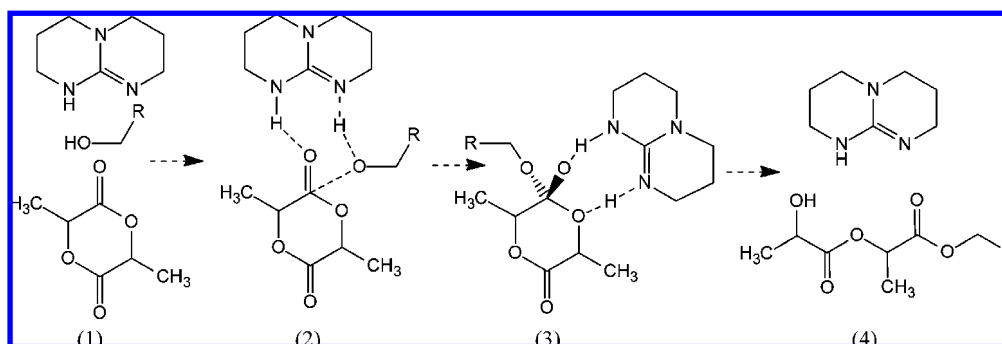
(1) Dechy-Cabaret, O.; Martin-Vaca, B.; Bourissou, D. *Chem. Rev.* **2004**, *104*, 6147.

(2) Csihony, S.; Culkin, D. A.; Sentman, A. C.; Dove, A. P.; Waymouth, R. M.; Hedrick, J. L. *J. Am. Chem. Soc.* **2005**, *127*, 9079.

(3) Dove, A. P.; Pratt, R. C.; Lohmeijer, B. G. G.; Waymouth, R. M.; Hedrick, J. L. *J. Am. Chem. Soc.* **2005**, *127*, 13798.

(4) Pratt, R. C.; Lohmeijer, B. G. G.; Long, D. A.; Waymouth, R. M.; Hedrick, J. L. *J. Am. Chem. Soc.* **2006**, *128*, 4556.

(5) Lohmeijer, B. G. G.; Pratt, R. C.; Leibfarth, F.; Logan, J. W.; Long, D. A.; Dove, A. P.; Nederberg, F.; Choi, J.; Wade, C.; Waymouth, R. M.; Hedrick, J. L. *Macromolecules* **2006**, *39*, 8574.

**Scheme 1.** Dual Activation of Monomer and Initiator by TBD**Scheme 2.** Dual Activation by TBD Strictly through Hydrogen Bonding

proposed for the bifunctional thiourea amine catalyzed ROP,<sup>3</sup> and also consistent with Berkessel's demonstration of the dynamic kinetic resolution of azlactones using urea-based chiral bifunctional catalysts, where the thiourea group was involved in hydrogen bonding to the carbonyl of the azlactone.<sup>6</sup> The mechanism was reported to involve simultaneous activation of the carbonyl group through hydrogen bonding (to the thiourea) along with activation of the initiating alcohol through interaction with a pendant tertiary amine.<sup>3</sup> In the first step of this scheme, the hydrogen attached to the nitrogen of TBD activates the carbonyl group of the L-lactide through hydrogen bonding, and the imine nitrogen simultaneously activates the alcohol by attracting the hydrogen of its hydroxyl group through a lone pair interaction (2). This results in an intermediate (3) with a tetrahedral center at the carbon of this carbonyl group. The catalyst then effects the subsequent ring opening by continuing to hydrogen bond to the oxygen of the carbonyl group, but now transferring the hydrogen (originally from the alcohol) to the ring oxygen adjacent to the carbonyl group (3).

### Calculation Details

Geometries were optimized for all reactants, transition states, and products depicted on the reaction profiles in Figures 1 and 2 using MPW1K density functional theory<sup>7</sup> and a 6-31+g\* basis set<sup>8</sup> in the presence of dichloromethane, which was modeled by the

continuum dielectric (c-PCM) method.<sup>9</sup> (Only electrostatics were included in the PCM calculations.) Frequencies were calculated for all transition states, and it was verified that there was only one imaginary frequency corresponding to the vibrational mode along the reaction coordinate. Energies were then calculated using MPW1K and the aug-ccpVTZ basis<sup>10</sup> at the MPW1K/6-31g+\* geometry. The GAMESS/US Quantum Chemistry package<sup>11</sup> was used for all calculations. The alcohol was modeled by methanol and TBD by guanidine in the generation of the full reaction profiles of both schemes (see Figures 1 and 2). The rate-determining step of each scheme was then re-examined using TBD as the catalyst.

### Results and Discussion

Considering first Scheme 1, the barrier height for the initial step, nucleophilic attack by the imine nitrogen of the guanidine at the carbonyl carbon of the L-lactide, is 8.8 kcal/mol, suggesting a plausible mechanism if this is indeed the rate-determining step. However, both the second step, ring opening of the lactide, and the third step, attack of the alcohol at the carbonyl carbon of the imide bond, have significantly higher barrier heights: 18.9 and 23.5 kcal/mol, respectively.

Looking more closely at the mechanism in Figure 1, just prior to TS2, we see the intermediate where the guanidinium moiety has rotated in order for the hydrogen to be ready to migrate to the oxygen adjacent to the carbonyl group. In TS3, the proton

(6) (a) Berkessel, A.; Mukherjee, S.; Cleeman, F.; Muller, T. N. *Chem. Commun.* **2005**, 1898. (b) Berkessel, A.; Mukherjee, S.; Cleemann, F.; Muller, T. N. *Angew. Chem., Int. Ed.* **2005**, *44*, 807.

(7) Lynch, B. J.; Fast, P. L.; Harris, M.; Truhlar, D. G. *J. Phys. Chem. A* **2000**, *104*, 21.

(8) (a) Hehre, W. J.; Ditchfield, R.; Pople, J. A. *J. Chem. Phys.* **1972**, *56*, 2257. (b) Hariharan, P. C.; Pople, J. A. *Theor. Chim. Acta* **1973**, *28*, 213. (c) Clark, T.; Chandrasekhar, J.; Spitznagel, G. W.; Schleyer, P. v. R. *J. Comput. Chem.* **1983**, *4*, 294.

(9) (a) Barone, V.; Cossi, M. *J. Phys. Chem. A* **1998**, *102*, 1995. (b) Cossi, M.; Rega, N.; Scalmani, G.; Barone, V. *J. Comput. Chem.* **2003**, *24*, 669.

(10) (a) Woon, D. E.; Dunning, T. H., Jr. *J. Chem. Phys.* **1995**, *103*, 4572. (b) Kendall, R. A.; Dunning, T. H., Jr.; Harrison, R. J. *J. Chem. Phys.* **1992**, *96*, 6796.

(11) Schmidt, M. W.; Baldridge, K. K.; Boatz, J. A.; Elbert, S. T.; Gordon, M. S.; Jensen, J. H.; Koseki, S.; Matsunaga, N.; Nguyen, K. A.; Su, S. J.; Windus, T. L.; Dupuis, M. M.; Montgomery, J. A. *J. Comput. Chem.* **1993**, *14*, 1347. (<http://www.msg.ameslab.gov/GAMESS/GAMESS.html> (R5))

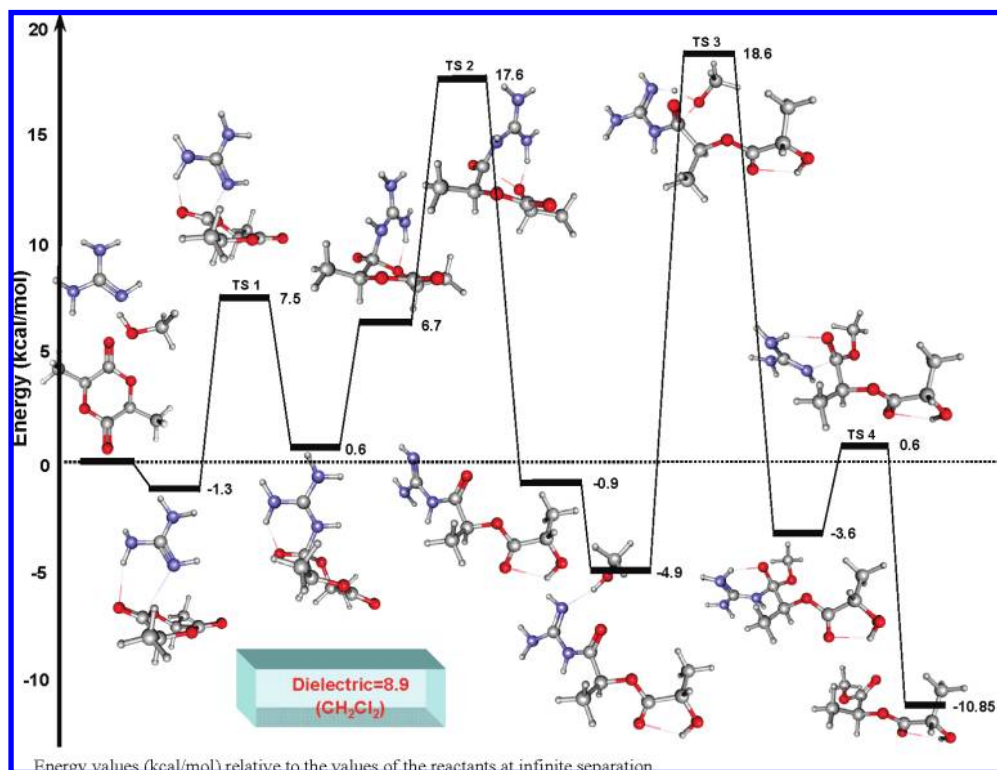


Figure 1. Energy profile for Scheme 1.

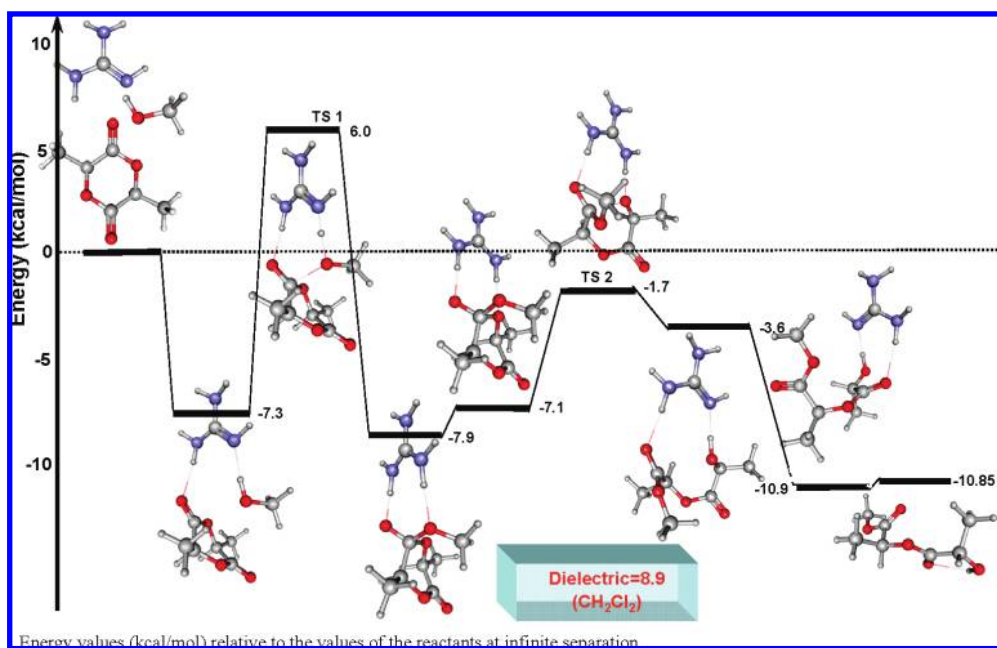
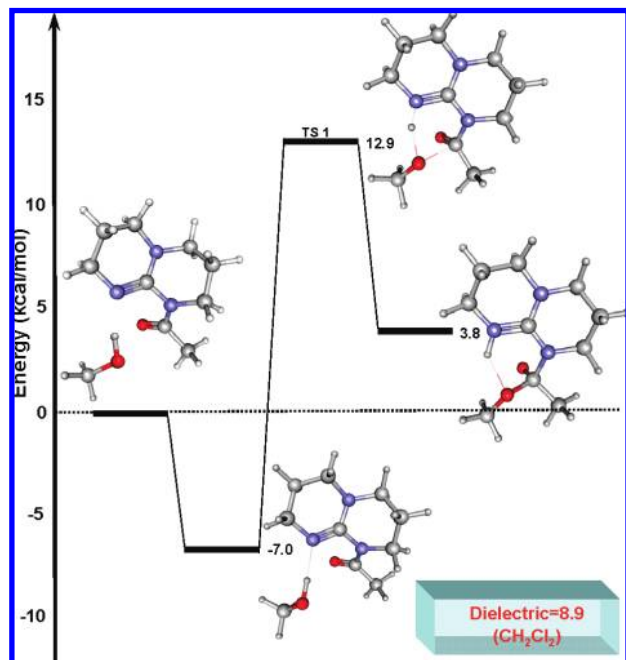


Figure 2. Energy profile for Scheme 2.

migrates from the alcohol to the guanidine moiety, activating the alcohol, and there is a hydrogen bond stabilization in the resulting intermediate between this migrated hydrogen and the oxygen of the carbonyl group (distance = 1.74 Å). Release of the catalyst in step 4 is then relatively easy with a much lower barrier of 4.2 kcal/mol. Note that both TS2 and TS3 have six-membered rings involving the bonds that are breaking and forming.

The high barrier of 23.5 kcal/mol for step 3 of Scheme 1, makes this the rate-determining step for Scheme 1. As expected,

this step does correspond to approach of the alcohol along a Burgi–Dunitz trajectory as evidenced by the geometry of TS3. (The reactant conformation for this step does not show this arrangement since such a conformation is not a minimum on the potential energy surface. Rather, this conformation is adopted along the path to the transition state.) In order to investigate this step further, we decided to reduce the complexity of the calculations and considered *N*-acetylguanidine as a surrogate for *N*-lactylguanidine. The barrier calculated for *N*-acetylguanidine was only 0.9 kcal/mol different from that for *N*-lac-



**Figure 3.** Effect of modeling *N*-acetylTBD rather than by simplifying with *N*-acetylguanidine in calculation of step 3 of Scheme 1.

tylguanidine (see Figure S1 in Supporting Information), supporting this simplification. We then considered the effect of the full catalyst and replaced *N*-acetylguanidine by *N*-acetylTBD. The profile for the corresponding reaction is given in Figure 3 and should be compared with that for step 3 of Scheme 1/Figure 1. Examination shows that TBD reduces the barrier height to 19.9 kcal/mol, a drop of 3.6 kcal/mol that can be attributed to the stronger basicity of TBD relative to guanidine. (The  $pK_a$  of the conjugate acid of TBD is 26 compared to the corresponding value of 12.5 for guanidine.) For TBD, this increased basicity results in an additional stabilization of 2 kcal/mol for the reactant complex, but this is more than compensated for by the increased activation of the alcohol in the transition state where the Lowdin charge on the oxygen atom of the alcohol is  $-0.82$  compared to  $-0.77$  in the *N*-acetylguanidine-catalyzed reaction, resulting in a lower barrier height.

Let us now turn to Scheme 2, the hydrogen-bonded mechanism. On examination of Figure 2, we see that the rate-determining step corresponds to the first step: catalyzed, activated attack of the alcohol on the carbonyl group of the lactide with a barrier of 13.3 kcal/mol (step 1). The catalyst then rearranges after formation of the initial intermediate so that it now hydrogen bonds to the oxygen adjacent to the carbonyl group (H bond distance = 1.88 Å), as well as to the oxygen of the carbonyl group itself (distance = 1.58 Å). This facilitates the opening of the ring, and the hydrogen migrates back from the guanidinium to form the alcohol. The lowest conformer of the chain is then 7.3 kcal/mol more stable than the conformer resulting directly from the transition state.

The rate-determining step, step 1, is somewhat analogous to step 3 of Scheme 1 in the sense that the methanol is again approaching along a Burgi–Dunitz trajectory and the intermediate that results has a tetrahedral carbon center with a lengthened carbonyl bond. However, in step 3 of Scheme 1, the catalyst is constrained by the covalent bond to the lactyl moiety, whereas in the transition state for step 1 of Scheme 2 the catalyst is less

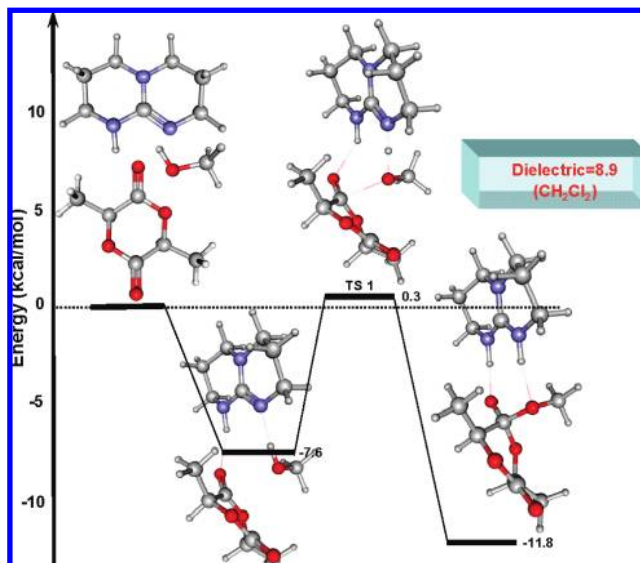
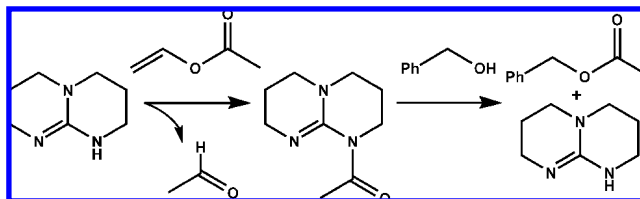


**Figure 4.** Reaction profile for step 1 of Scheme 2 using TBD as catalyst.

### Scheme 3. Acyl Transfer Reaction



constrained and can additionally hydrogen bond to the oxygen of the carbonyl group, which serves to stabilize the transition state.

The highest barrier of 13.3 kcal/mol is reduced to 7.9 kcal/mol when TBD replaces guanidine as the catalyst (see Figure 4). This energy reduction is due almost entirely to stabilization of the transition state since, in both the TBD and guanidine case, the reactant complex is stabilized by around 7 kcal/mol relative to separate reactants. In the TBD transition state, the Lowdin charge on the oxygen is again  $-0.8$ , but in this transition state, the hydrogen on the N–H group of the TBD is able to hydrogen bond to the carbonyl oxygen on the lactide. Note that the transition state has a loosely bound eight-membered ring, in line with the most stable transition state found for methanolysis of  $\epsilon$ -caprolactone.<sup>12</sup> This is in contrast to step 3 of Scheme 1 that has a six-membered ring transition state and no hydrogen available to hydrogen bond to the oxygen of the carbonyl group. Overall, these effects result in the rate-determining step of Scheme 2 having a significantly lower barrier than that for Scheme 1. The difference of 12 kcal/mol between the barriers for the rate-determining steps of Scheme 1 and Scheme 2 supports Scheme 2 as the likely mechanism—a fact that is illustrated even in the idealized model reaction with guanidine depicted in Figures 1 and 2, where the corresponding difference is 10 kcal/mol.

The possibility of catalysis through a hydrogen-bonded mechanism is further supported by experimental work on related reactions. Corey's study of bicyclic guanidine catalysts in the

(12) Buis, N.; French, S. A.; Ruggiero, G. D.; Stengel, B.; Tulloch, A. A. D.; Williams, I. H. *J. Chem. Theory Comput.* **2007**, 3, 146.



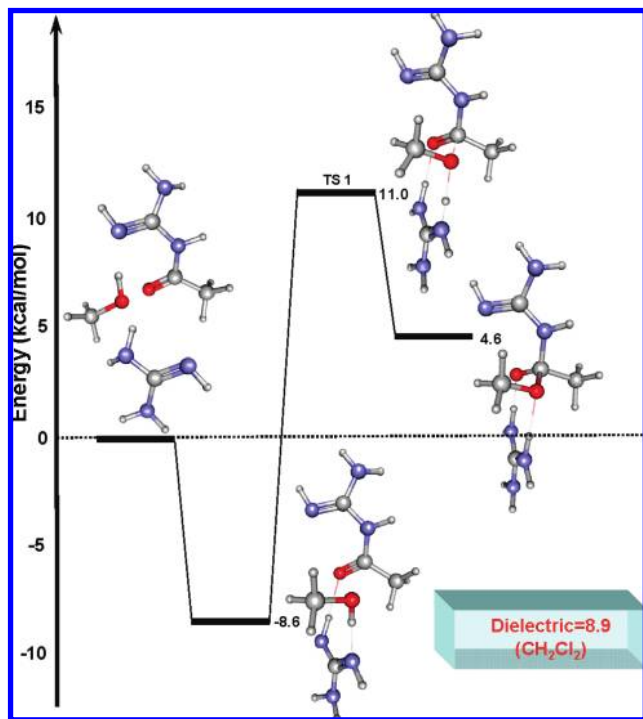
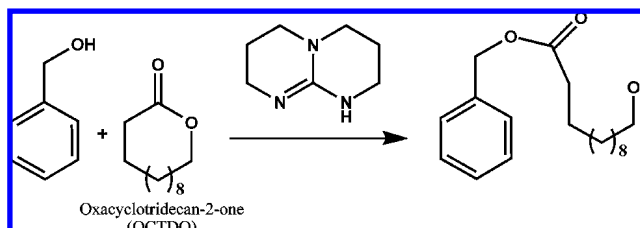


Figure 5. Effect of additional catalyst molecule on step 3 of Scheme 1.

enantioselective Strecker synthesis of  $\alpha$ -aminonitriles and  $\alpha$ -amino acids showed that bicyclic guanidine catalysts can exhibit bifunctional hydrogen bonding capability.<sup>13</sup> Furthermore, it has been demonstrated that addition of malonic esters to nitro-olefins can be catalyzed by both TBD<sup>14</sup> and a bifunctional urea,<sup>15</sup> suggesting that there may well be a similar mechanism for both reactions.

In earlier work,<sup>4</sup> Scheme 1 was postulated as the reaction mechanism due to analysis of the ease of the reaction depicted in Scheme 3. In the first step of this reaction, *N*-acetylTBD is formed and isolated after reaction of TBD with vinyl acetate. In a second step, benzyl alcohol reacts with the *N*-acetylTBD to give benzyl acetate, liberating TBD. This second step is directly analogous to step 3 of Scheme 1 and does not appear at first sight to be facile from the calculated barrier height of 19.9 kcal/mol for *N*-acetylTBD reacting with methanol (depicted in Figure 3). However, the reaction in step 2 of Scheme 3 was performed with considerably higher concentrations of *N*-acetylTBD and alcohol than the ring-opening polymerization reaction. In fact, the concentrations of *N*-acetylTBD and alcohol were 0.33 and 1.77 mol/L, that is, 470 and 240 times larger for this reaction than for the catalytic ROP reaction, respectively. Assuming that the reaction is linear in both TBD and alcohol concentrations, increasing the concentrations by these factors is effectively equivalent to reducing the barrier height by 6.9 kcal/mol at catalytic concentrations. Given the higher concentration of reactants, we took the model reaction of acetylguanidine with methanol for this step and also considered the possibility that a second catalyst molecule could be involved in step 2 (see Figure 5). This catalyst molecule can now hydrogen bond to the oxygen of the carbonyl group and form an eight-membered

Scheme 4. Ring-Opening Reaction of OCTDO with Benzyl Alcohol (BAol) as Initiator and TBD as Catalyst



ring transition state (rather than a six-membered ring, Figure 5). By so doing, the barrier was reduced by 4.8 kcal/mol. The higher concentrations of reactants and the possibility that a second catalyst molecule can be involved in the mechanism now makes step 2 of reaction 3 more feasible than its counterpart, step 3 of Scheme 1, and thus could explain why Scheme 3 is quite plausible, but yet the hydrogen-bonded mechanism is the likely pathway for the catalytic ring-opening polymerization. This conclusion hinges on the fact that rate-determining steps for each scheme are properly modeled by the calculations. In order to test this, experimental kinetic studies were done to elucidate the order of the reaction. NMR was used to study the reaction order of the ring-opening reaction of oxacyclotridecan-2-one (OCTDO) with benzyl alcohol (BAol) as initiator and TBD as catalyst (see Scheme 4). OCTDO was chosen as the target cyclic ester due to its relatively low reactivity with alcohol with TBD catalyst, so that the reaction rate was appropriate for NMR testing (experimental details are given in the Supporting Information).

The experimental results are shown in Figure 6. Note that line 1 shows a linear correlation between  $\ln(\text{conversion of BAol})$  and time, indicating a pseudo-first-order reaction to BAol. Line 2 demonstrates a similar linear correlation between  $\ln(\text{conversion of OCTDO})$  and time, indicating first-order reaction to OCTDO. Line 3 again demonstrates linear correlation between  $\ln(\text{conversion of OCTDO})$  and time, indicating the first-order reaction to OCTDO. The ratio of the slope of line 3,  $k_3$ , to the slope of line 2,  $k_2$ , is equal to the ratio of the concentration of TBD in the two systems, supporting a first-order reaction to TBD. Taken

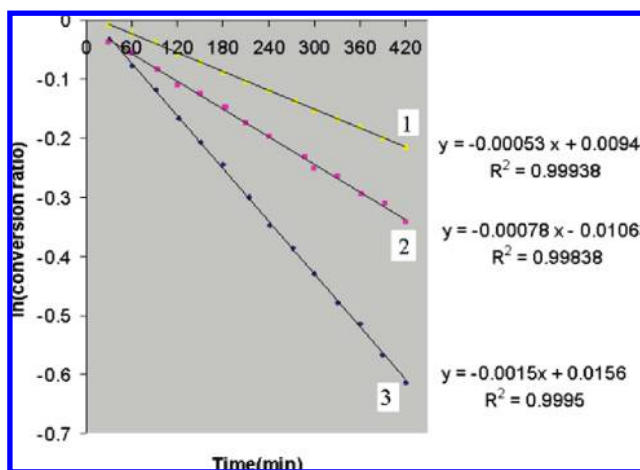


Figure 6. Experimental results. Line 1: 10.0 mg of TBD + 20 mg of OCTDO + 1.0  $\mu\text{L}$  of BAol in 0.53 g of toluene- $d_8$  (large excess of TBD and OCTDO relative to BAol). Line 2: 5.0 mg of TBD + 21.6 mg of BAol + 1.0  $\mu\text{L}$  of OCTDO in 0.50 g of toluene- $d_8$  (large excess of TBD and BAol relative to OCTDO). Line 3: 10.0 mg of TBD + 21.5 mg of BAol + 1.0  $\mu\text{L}$  of toluene- $d_8$  (large excess of TBD and BAol relative to OCTDO).

(13) Corey, E. J.; Grogan, M. J. *Org. Lett.* **1999**, *1*, 157.

(14) Ye, W.; Xu, J.; Tan, C.-T.; Tan, C.-H. *Tetrahedron Lett.* **2005**, *46*, 6875.

(15) Okino, T.; Hoashi, Y.; Furukawa, T.; Xu, X.; Takemoto, Y. *J. Am. Chem. Soc.* **2005**, *127*, 119.

together, these results support an overall third-order reaction: first-order with respect to alcohol concentration, first-order with respect to catalyst concentration, and first-order with respect to lactone concentration. This rules out step 1 of Scheme 1 being the rate-limiting step (in agreement with the computational results) and is consistent with step 1 of Scheme 2 or step 3 of Scheme 1 being the rate-limiting step. On the basis of the large difference of 12 kcal/mol found (computationally) between the barrier heights of step 3 of Scheme 1 and step 1 of Scheme 2, we thus favor the hydrogen bonding mechanism (Scheme 2).

## Conclusions

This study illustrates the importance of hydrogen bonding in the organocatalytic ring opening reaction of L-lactide and favors a reaction mechanism based entirely on hydrogen bonding to the catalyst rather than a mechanism based on acetyl transfer. What are the ramifications of the hydrogen bonding mechanism? Clearly, the rate would be slower if no hydrogen bonding agent were present, and this is borne out by the fact that the rate of ROP of L-lactide is more than 90 times slower with methyl TBD than with TBD itself.<sup>4</sup> The reaction mechanism is pseudoanionic in the sense that the catalyst, TBD, activates the alcohol by attracting its proton. This kind of activation will be stabilized in more polar solvents albeit with the caveat that there is no competing interaction between the polar solvent and TBD, tying up the TBD and stopping it from interacting with the alcohol. Finally, any catalyst that can further help stabilize the tetrahedral carbon center in the transition state of the rate-determining step

(step 1 of Scheme 2) would be an advantage. Clearly the hydrogen bonding of the TBD to the carbonyl oxygen is aiding in this respect; the C–O bond is 1.202 Å in the transition state, compared with 1.119 Å in L-lactide, indicative of more single bond character in the transition state. In the case of the ROP of L-lactide by thiourea, there are two sites available to hydrogen bond to the carbonyl oxygen of L-lactide,<sup>3</sup> so designing a catalyst that has this double hydrogen-bonded functionality could be an advantage. Finally, an alcohol with a less bulky side chain may also be beneficial since a large bulky side chain could destabilize the transition state through steric hindrance.

**Note Added after Submission.** The results generated independently by Simon and Goodman (*J. Org. Chem.* **2007**, *72*, 9656) perform a similar analysis for the TBD-catalyzed ring opening of  $\epsilon$ -caprolactone and also come to the conclusion that the hydrogen bonding mechanism is favored.

**Acknowledgment.** The authors appreciate stimulating discussions with the groups of Dr. Jim Hedrick and Prof. Bob Waymouth, as well as funding from CPIMA under NSF-MRSEC (Grant #DMR-0213618).

**Supporting Information Available:** Experimental details, Figure S1, and coordinates of all stationary point structures in xyz format. This material is available free of charge via the Internet at <http://pubs.acs.org>.

JA0764411